

ELECTROMAGNETIC RADII OF H^3 AND He^3

R. H. Dalitz and T. W. Thacker

Clarendon Laboratory, Oxford, England

(Received 7 July 1965)

The form factors for the charge structure and the magnetic-moment structure of H^3 and He^3 have recently been determined from elastic electron scattering experiments by Collard *et al.*¹ The most striking result was that the rms radii and form factors for the H^3 and He^3 charge distributions are substantially different, the rms radii for the proton distributions being

$$a(\text{H}^3) = 1.47 \pm 0.07 \text{ F}, \quad a(\text{He}^3) = 1.66 \pm 0.07 \text{ F}. \quad (1)$$

The ratio $F_{\text{ch}}(\text{H}^3)/F_{\text{ch}}(\text{He}^3)$ of their charge form factors deviates considerably from unity and is plotted in Fig. 1 as a function of q^2 . The magnetic-moment radii for H^3 and He^3 are comparable with the H^3 charge radius, $a_{\text{ch}}(\text{H}^3) = 1.70 \pm 0.05 \text{ F}$, as indicated by the entries a_{mag} in Table I.

This difference between the charge radii for H^3 and He^3 has excited much discussion, since it reflects a significant lack of spatial symmetry between the three nucleons in the three-

nucleon doublet. However, Schiff² has pointed out that there exists a simple origin for an asymmetry between the three nucleons in these systems, namely that the unlike nucleon has a binding energy greater by $B_D = 2.236 \text{ MeV}$ than that for the like nucleons. The charge radius measured for He^3 refers to the less tightly bound like nucleons, whereas that for H^3 refers to the more tightly bound unlike nucleon; in fact, the binding of the unlike nucleon in H^3 is already 0.76 MeV greater than that for the unlike nucleon in He^3 , owing to the Coulomb energy of He^3 . Since the rms radius is particularly sensitive to the outer region of the nucleus, just where the nucleon wave functions are governed mainly by their binding energies, this interpretation of the difference $[a(\text{He}^3) - a(\text{H}^3)]$ appears exceedingly plausible, and it appears reasonable to expect this difference to be insensitive to the details of the interior wave function. However, there does not appear to be any quantitative estimate of this effect in the literature. In this Letter, our purpose is to consider the effects of this binding-energy asymmetry of the rms radii of H^3 and He^3 , and to show that this asymmetry appears quite capable of accounting for the differences observed.

First, we consider a simple model (see Fig. 2). We suppose that, in these systems, the wave function $\Psi(r)$ of a nucleon (where r denotes its distance from the center of mass) consists of two parts: (i) a central region $r \leq R$ where Ψ has the same form for all nucleons, for both H^3 and He^3 , say $\Psi = C$, for simplicity, and (ii) the outer region $r \geq R$ where the form of $\Psi(r)$ is controlled by the binding energy B of the nucleon it describes, so that

$$\Psi(r) = (CR/r) \exp[-\lambda(r-R)], \quad r \geq R, \quad (2)$$

where $\lambda = \frac{3}{2}(2M_{\text{red}}B)^{1/2}$ and M_{red} is the reduced mass (essentially $2M/3$) of the nucleon. The rms radius of the nucleon distribution is then given by

$$a = R \left(\frac{3}{5} \right)^{1/2} \left\{ \frac{2 + 5x + 5x^2 + (5/2)x^3}{2 + 3x} \right\}^{1/2}, \quad (3)$$

where $x = (\lambda R)^{-1}$. The radius R may be deter-

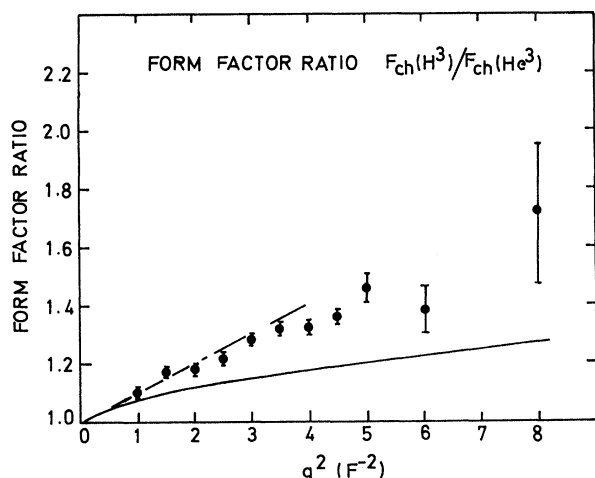


FIG. 1. The form factor ratio $F_{\text{ch}}(\text{H}^3)/F_{\text{ch}}(\text{He}^3)$ obtained by Collard *et al.*¹ from their electron scattering experiments is plotted as a function of q^2 , where q denotes the momentum transfer. The solid curve shows the ratio calculated here for the naive model depicted in Fig. 2, the deviation of this ratio from unity being due to the difference between the proton binding energies in H^3 and He^3 . The dashed line through the origin has the slope appropriate to the rms charge radii for H^3 and He^3 , being of the form $\frac{1}{6}q^2[a^2(\text{He}^3) - a^2(\text{H}^3)]$.

Table I. The rms radii $a(\text{H}^3)$ and $a(\text{He}^3)$ for the proton mass distributions in H^3 and He^3 and the rms magnetic-moment radii $a_{\text{mag}}(\text{H}^3)$ and $a_{\text{mag}}(\text{He}^3)$ are compared with the values calculated with the naive model depicted in Fig. 2, with the modified Pappademos wave function (7) with $F(\alpha, r)$ given by (6), which is identical with the wave function (7) with (10) for $z = 1.0$, and with the wave function (7) with $F(\alpha, r)$ given by (10).

	Experimental values (F)	Naive model (Fig. 2)	Modified Pappademos wave function $z = 1.00$	Wave function (7) with $F(\alpha, r)$ given by (10) $z = 1.25; z = 1.50$	
$a(\text{H}^3)$	1.47 ± 0.07	1.49	1.66	1.53	1.42
$a(\text{He}^3)$	1.66 ± 0.07	1.66	1.88	1.73	1.59
$a_{\text{mag}}(\text{H}^3)$	1.70 ± 0.05	1.71	1.84	1.73	1.63
$a_{\text{mag}}(\text{He}^3)$	1.74 ± 0.10	1.73	1.91	1.79	1.68

mined by equating (3) with $a(\text{He}^3)$, using $B = 5.49$ MeV, and so $\lambda = 0.631 \text{ F}^{-1}$; this leads to $R = 0.939 \text{ F}$. For H^3 , the only change is in the asymptotic form (2), corresponding to $B = 8.48$ MeV and $\lambda = 0.780 \text{ F}^{-1}$. With these parameters, expression (3) leads to $a(\text{H}^3) = 1.50 \text{ F}$, in excellent agreement with the observed value. Further, with this naive model, the form factor for the nucleon distribution is given by

$$F(q) = \left\{ 3 \frac{\sin qR - qR \cos qR}{(qR)^3} - \frac{3 \exp(2\lambda R)}{qR} \times \text{Im}[Ei(-2\lambda R + iqR)] \right\} / \left\{ 1 + \frac{3}{2\lambda R} \right\}. \quad (4)$$

Here, we are interested in the dependence of $F(q)$ on the proton binding energy B , rather

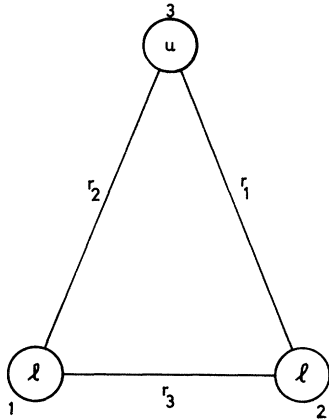


FIG. 2. The nucleon wave function used for the naive-model discussion given here of the relation of the various rms radii for H^3 and He^3 with the binding energies of their like and unlike nucleons. The interior wave function (for $r \leq R$) is assumed the same for all nucleons, while the exterior wave function (for $r \geq R$) is controlled by the nucleon binding energy, the parameter λ being given by $\frac{3}{2}(2M_{\text{red}}B)^{1/2}$.

than in the absolute fit with the observed form factors, and so we compare the calculated ratio $F(\text{H}^3, q)/F(\text{He}^3, q)$, given by the solid curve in Fig. 1, with the empirical data. Although not in precise agreement with the data, the deviation of this ratio from unity is quite comparable with the deviation observed, and shows the same trend with increasing q^2 . It appears at least that a large part of the form-factor difference can be quite well understood in terms of the binding-energy difference.

Assuming that the magnetic-moment distributions arise only from the unlike nucleon, the rms magnetic radii are $(a^2 + a_p^2)^{1/2}$, where a denotes the rms radius for the neutron distribution in He^3 and for the proton distribution in H^3 . Thus, we expect $a_{\text{mag}}(\text{H}^3) = a_{\text{ch}}(\text{H}^3)$, and also $a_{\text{mag}}(\text{He}^3) \approx a_{\text{mag}}(\text{H}^3)$, since the neutron binding energy in He^3 is 7.72 MeV. The magnetic radii calculated are given in Table I and are in good agreement with this expectation and with the data.

Next, we extend these considerations to a more realistic wave function based on that used at an earlier stage by Pappademos³ in his discussion of the rms radius and Coulomb energy of He^3 ,

$$\Psi = F(\alpha, r_1)F(\alpha, r_2)F(\alpha, r_3)\chi_{1/2}, \quad (5)$$

where $\chi_{1/2}$ denotes the $S = \frac{1}{2}$ spin wave function,

$$F(\alpha, r) = \{\exp[-\alpha(r-d)] - \exp[-\beta(r-d)]\}r^{-1/2}, \quad (6)$$

and d denotes the hard core radius of the NN potential, taken here as $d = 0.5 \text{ F}$ on the basis of the experience of Breit and coworkers⁴ in fitting semiphenomenological potentials to the nucleon-nucleon scattering data. The value $\beta = 5.5 \text{ F}^{-1}$ was determined by Pappademos from the requirement that $F(\alpha, r)$ reproduce the form of the two-nucleon wave function at

short distances, as argued by Dalitz and Downs⁵ and Austern and Iano.⁶ The parameter α was determined directly from the mean nucleon binding energy. In order to allow for the non-symmetry of the asymptotic wave function which follows from the binding-energy differences, we replace the wave function (5) by

$$\chi = F(\alpha_u, r)F(\alpha_u, r)F(\alpha_l, r)\chi_{1/2}, \quad (7)$$

where the suffices l, u refer to the like and unlike pairs, respectively (cf. Fig. 3). From the asymptotic form of (7), the parameters α_u and α_l are given by

$$2\alpha_u = (2M_{\text{red}}B_u)^{1/2}, \quad \alpha_u + \alpha_l = (2M_{\text{red}}B_l)^{1/2}. \quad (8)$$

Their values are $\alpha_u = 0.260 \text{ F}^{-1}$, $\alpha_l = 0.188 \text{ F}^{-1}$ for H^3 , and $\alpha_u = 0.249 \text{ F}^{-1}$, $\alpha_l = 0.172 \text{ F}^{-1}$ for He^3 . The rms matter radii are calculated using the expressions

$$a_u^2 = \frac{1}{9}(2r_1^2 + 2r_2^2 - r_3^2), \quad (9a)$$

$$a_l^2 = 1/18(r_1^2 + r_2^2 + 4r_3^2), \quad (9b)$$

with the results given in Table I. The value $[a(\text{He}^3) - a(\text{H}^3)] = 0.22 \text{ F}$ agrees well with the observed difference, in support of the qualitative arguments given above. The calculated radius $a_{\text{mag}}(\text{He}^3)$ is only 0.04 F larger than $a_{\text{mag}}(\text{H}^3)$, in accord with the empirical difference $0.04 \pm 0.11 \text{ F}$.

However, all the radii calculated with the wave function (5) are about 10% larger than the observed radii. We attribute this to the fact that the form (6) used for $F(\alpha, r)$ satisfies $F(\alpha, r) \leq \exp[-\alpha(r-d)]/(r)^{1/2}$ at all radii, so that the concentration of this wave function at short distances cannot be arbitrarily large. This defect can be removed by using a more flexible form for $F(\alpha, r)$:

$$F(\alpha, r)$$

$$= \{[\exp(-\alpha(r-d)) - \exp(-\gamma(r-d))]\} \\ + z[\exp(-\gamma(r-d)) - \exp(-\beta(r-d))]\}r^{-1/2}, \quad (10)$$

consisting of two independent terms, the first dominating the asymptotic region, the second dominating at short distances. In order to illustrate the effect of this flexibility, the intermediate value $\gamma = 1.0 \text{ F}^{-1}$ has been chosen.

As a guide to reasonable values for z , $F(\alpha, r)$ has been compared with the deuteron wave function given by Moravcsik⁷ over the range 0.75

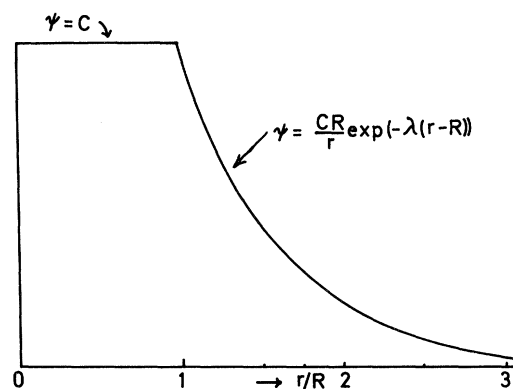


FIG. 3. The coordinate system used for the three-nucleon wave function (7) discussed here. Nucleons 1 and 2 are the like nucleons (l), and nucleon 3 is the unlike nucleon (u).

to 3.0 F [the asymptotic form of (10) would not be correct for the deuteron, of course], giving the estimate $z = 1.25$. The value of z appropriate to the three-nucleon systems need not be the same as for the deuteron, but is not expected to be widely different. The rms radii calculated with (7) and (10) are listed in the table for $z = 1.0, 1.25$, and 1.5 ; the observed value for $a(\text{He}^3)$ corresponds to the reasonable choice $z = 1.375$. For this choice of z , $a(\text{H}^3) = 1.47 \text{ F}$, corresponding to a difference $[a(\text{He}^3) - a(\text{H}^3)] = 0.19 \text{ F}$, in complete agreement with the data. The magnetic radius $a_{\text{mag}}(\text{He}^3)$ is 0.07 F larger than $a_{\text{mag}}(\text{H}^3)$, again in satisfactory agreement with the data.

To conclude, the calculations described above and summarized in Table I show that the binding-energy asymmetry pointed out by Schiff appears quite capable of accounting for the differences observed empirically between the charge and magnetic-moment radii of H^3 and He^3 . Although the form factors have not yet been evaluated for the realistic wave function (7), the ratio of the charge form factors for He^3 and H^3 obtained from the naive model of Fig. 2 shows an encouraging qualitative accord with the experimental ratio.

One of us (T.W.T.) wishes to acknowledge here the support of a maintenance grant from the Department of Scientific and Industrial Research.

¹H. Collard, R. Hofstadter, E. B. Hughes, A. Johansson, M. R. Yearian, R. B. Day, and R. T. Wagner, Phys. Rev. **138**, B59 (1965).

²L. I. Schiff, Phys. Rev. **133**, B802 (1964).

³J. N. Pappademos, Nucl. Phys. **42**, 122 (1963); **56**, 351 (1964).

⁴These fits require values of the hard-core radius within the range 0.50 ± 0.03 F. We are indebted to Dr.

M. Hull for a discussion concerning this point.

⁵B. W. Downs and R. H. Dalitz, Phys. Rev. **114**, 593 (1959).

⁶N. Austern and P. Iano, Nucl. Phys. **18**, 672 (1960).

⁷M. J. Moravcsik, Nucl. Phys. **1**, 113 (1958).

FURTHER EVIDENCE FOR A POSSIBLE $I=\frac{5}{2}$ N^* RESONANCE AT 1580 MeV

G. Alexander, O. Benary, B. Reuter, A. Shapira, E. Simopoulou, and G. Yekutieli

Nuclear Physics Department, The Weizmann Institute of Science, Rehovoth, Israel

(Received 17 June 1965)

In a study of the reaction $\pi^+ + p \rightarrow p + \pi^+ + \pi^+ + \pi^-$ at 3.65 GeV/c, Goldhaber et al.¹ have reported on an enhancement seen in the $p\pi^+\pi^+$ -invariant mass distribution at 1.56 ± 0.02 GeV with a width of $\Gamma = 0.20 \pm 0.02$ GeV, selecting small-momentum-transfer events of $\Delta^2(p\pi^+\pi^+) \leq 15m_\pi^2$. It was pointed out by the same authors that this enhancement, which may be due to the formation of an $I=\frac{5}{2}$ N^* resonance, could also be explained through the peripheral production of $\pi^+ + p \rightarrow N^{*++}(1238) + \rho^0$, taking into account the Bose symmetry of the two π^+ -mesons in the final state.

In the present work a search has been done in p - p collisions at 5.5 GeV/c at different final-state channels, looking for a possible formation of an $I=\frac{5}{2}$ N^* resonance. The work was carried out with 30 000 pictures taken with the 81-cm hydrogen bubble chamber at CERN exposed to a secondary beam of protons at 5.52 GeV/c. An unbiased sample of 1020 four-prong and 159 six-prong events have been measured and analyzed kinematically. A total of 1014 events yielded at least one kinematical fit, and most ambiguous events were resolved by the ionization method. The p - p reactions used in the present work, together with their cross-section values, are given in Table I.

The data have been analyzed in terms of resonance production as a function of their momentum transfer Δ^2 . As the initial state has two

identical particles, two values for the momentum transfer Δ^2 may be computed for each particle. However, the angular distribution of the final-state nucleons and nucleon-pion systems show a marked forward-backward peaking (see Fig. 1). We have therefore chosen from the two possible Δ^2 values the smaller one to represent the actual momentum transfer. This procedure is equivalent to a fold in the angular distribution through 90° .

The relative production rate of the different charge states of a possible $I=\frac{5}{2}$ N^* resonance and their subsequent $N\pi\pi$ decay configurations may be uniquely determined by isospin consideration in the reaction $p + p \rightarrow N_{5/2}^* + N + \pi$; $N_{5/2}^* \rightarrow N + \pi + \pi$. These relative production rates are given in Table II for Reactions (1) and (2). Final states of $NN\pi\pi$ involving more than one neutral particle could not be identified in the present work. As seen from Table II, the formation of an $I=\frac{5}{2}$ N^* resonance should mostly occur in the $p\pi^+\pi^+$ configuration of Reaction (1) and the $p\pi^+\pi^0$ configuration of Reaction (2). These two configurations have further the advantage that they cannot be in an $I=\frac{1}{2}$ state, and hence have no contribution from the two $I=\frac{1}{2}$ N^* resonances at 1.518 and 1.688 GeV. The invariant-mass distribution of $p\pi^+\pi^+$ and $p\pi^+\pi^0$ using all events shows some enhancement around 1580 MeV [Fig. 2(a)] which, however, is much more pronounced by using events with

Table I. Cross-section values for five- and six-body final states in pp collisions at 5.5 GeV/c.

	Reaction	No. of events	σ (mb)
(1)	$p + p \rightarrow n + p + \pi^+ + \pi^+ + \pi^-$	333	2.84 ± 0.15
(2)	$\rightarrow p + p + \pi^+ + \pi^- + \pi^0$	226	1.93 ± 0.13
(3)	$\rightarrow p + p + \pi^+ + \pi^+ + \pi^- + \pi^-$	74	0.63 ± 0.08